Geochimica Brasiliensis, 3(1): 63-80, 1989

PETROLOGICAL AND GEOCHEMICAL STUDIES OF ALKALINE ROCKS FROM CONTINENTAL BRAZIL. 8. THE SYENITIC INTRUSION OF MORRO REDONDO, RJ

P. Brotzu[1], L. Beccaluva[2], A. Conte[3], M. Fonseca[4], C. Garbarino[5], C.B. Gomes[6], R. Leong[6], G. Macciotta[7], R.L. Mansur[4], L. Melluso[1], L. Morbidelli[3], E. Ruberti[6], J.B. Sigolo[6], G. Traversa[8], J.G. Valença[4]

1. Dipartimento di Scienze della Terra, Università di Napoli, Italy
2. Istituto di Mineralogia, Università di Ferrara, Italy
3. Dipartimento di Scienze della Terra, Università di Roma "La Sapienza", Italy
4. Instituto de Geociências, Universidade Federal do Rio de Janeiro, Brazil
5. Istituto di Giacimenti Minerari, Università di Cagliari, Italy
6. Instituto de Geociências, Universidade de São Paulo, Brazil
7. Istituto di Scienze della Terra, Università di Catania, Italy
8. Dipartimento di Scienze della Terra, Università di Perugia, Italy

ABSTRACT

The alkaline complex of Morro Redondo is mainly composed of syenites, alkali syenites and nepheline syenites. The age of the intrusion, utilizing eleven newly available K/Ar data, is about 73 Ma. Petrography, mineral chemistry and geochemistry strongly support cogeneticity among the various lithotypes, linked by fractional crystallisation of the observed phases and crystal accumulation, preferentially of alkali feldspar.

Initial Sr isotopic ratios indicate a mantle parental magma, probably generated in the subcontinental lithosphere, like other Brazilian alkaline complexes (e.g. Fortaleza, Juquiá, Piratini, Tunas).

RESUMO

O complexo alcalino de Morro Redondo é constituído essencialmente de sienitos, álcali sienitos e nefelina sienitos. Onze determinações K/Ar recentemente obtidas indicam para a intrusão idade de 73 Ma. Evidências petrográficas, de química mineral e geoquímicas são fortemente indicativas do caráter cogenético dos vários tipos litológicos encontrados, com a sua formação se dando por cristalização fracionada das fases observadas e acumulação de cristais, preferencialmente de feldspato alcalino.

Razões isotópicas iniciais de Sr apontam para a natureza mantélica do magma parental dessas rochas, provavelmente gerado na litosfera subcontinental, a exemplo do sucedido com outros complexos alcalinos brasileiros (Fortaleza, Juquiá, Piratini, Tunas).

INTRODUCTION

The Morro Redondo alkaline complex, firstly described by Lamego (1936), is located about 160 km west of Rio de Janeiro, east of the larger complexes of Itatiaia and Passa Quatro. According to Valença *et al.* (1983), it is subcircular in plan and crops out over an area of 8 km^2, with sharp contacts against the gneissic Precambrian basement.

Poor exposure and diffuse superficial weathering preclude clear knowledge of the structure of the intrusion and of field relationships among the igneous rocks occurring in the area. The complex is composed of dominant medium- to coarse-grained nepheline syenites in the eastern, southern and northern sectors and by mostly altered phonolitic and trachytic breccias in the central-western part (Fig. 1); some fine-grained rocks, texturally related to border facies of the intrusion, crop out eastwards, near the contact with the basement and are also found as enclosed fragments in the nepheline syenites of the eastern sector. The nepheline syenites are cut by porphyritic or aphyric dykes with composition ranging from phonotephrite to peralkaline phonolite.

On the basis of field and petrographic evidences, Valença *et al.* (1983) claim the existence of mineral zoning for the whole syenitic mass, being the rocks from the central part of the complex, the higher topographically elevated areas, slightly enriched in nepheline and amphibole. Clinopyroxene and notably biotite represent the main femic phases in the lithotypes cropping out near the border of the intrusion.

More recently, the complex has been investigated from the petrological, geochemical and geochronological point of view within the Brazilian-Italian cooperative project dealing with alkaline rocks from continental Brazil, the preliminary results reported by Brotzu *et al.* (1988).

AGE

Eleven newly determined K/Ar data for the intrusive complex provide an age of about 73.6 Ma (Table 1, Fig. 2). Including the only available result from the literature (Ribeiro Filho & Cordani, 1966; 65.6 Ma, recalculated as 67.2 $\pm$ 4 Ma using the constants according to Steiger & Jaeger, 1977), age can be placed around 73.0 Ma. Absolute ages for the tephritic-phonolitic breccias are lacking, but field observations suggest later emplacement ages.

CLASSIFICATION AND PETROGRAPHY

The intrusive rocks of the complex are all distributed in the nepheline syenite field of the R1-R2 classificative diagram (De La Roche *et al.*, 1980; Fig. 3), except for the fine-grained border facies (22, 2) that plot near the essexite-nepheline syenite boundary. Taking into account the modal percentage of sialic minerals in the APF diagram (Streckeisen, 1976; Fig. 4), the intrusive coarse-grained rocks cover a range from plagiosyenites (22) to nepheline-bearing syenites (20, 27, 5, 4, 3, 23), alkali syenites (10, 9, 12, 11, 28) and nepheline syenites (14, 13, 16, 8, 1, 18, 26). The porphyritic and subaphyric dykes plotted in the R1-R2 diagram are classified as phonotephrites to phonolites (2, 7).

Microessexites, fine grained essexites or plagiosyenites, show varied textures from hypidiomorphic to autoallotriomorphic. Mineralogically, they are composed of nearly euhedral plagioclases and of corroded Ti-salitic clinopyroxene. Kaersutitic amphibole and biotite tend to develop

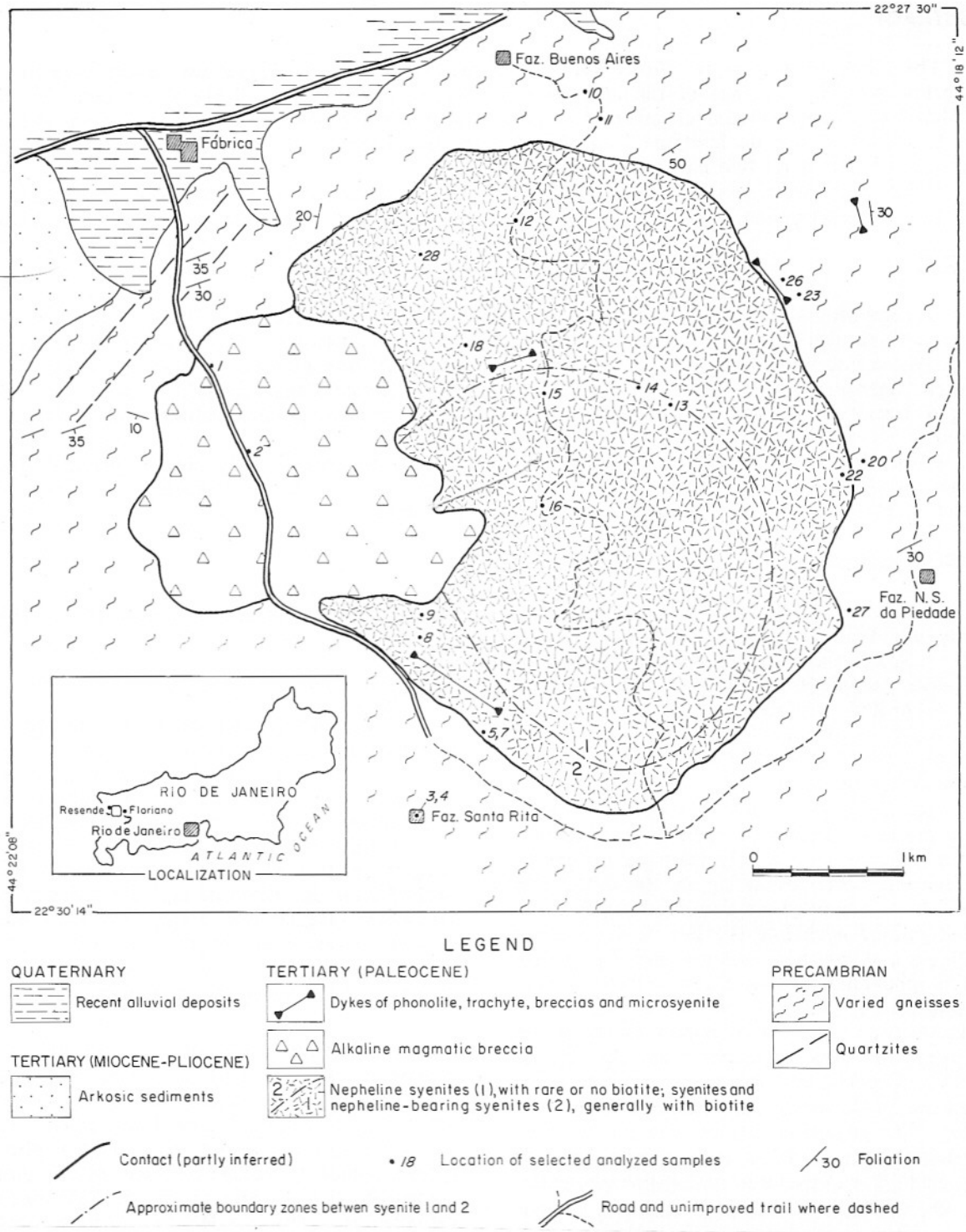

Figure 1 — Geological map of the alkaline complex of Morro Redondo. Resende, RJ (after Valença, J.G.; Reis, A.P.; Carvalho Filho, C.A.; Soares Filho, J.R.S.; Braun, P.B.C.B., unpublished).

poikilitically around the clinopyroxene; alkali feldspar and nepheline complete the paragenesis and are clearly interstitial phases. Apatite, Ti-magnetite and sphene are present as accessory phases of early crystallisation.

Nepheline-bearing syenites are medium- to coarse-grained rocks and are locally inequigranular due to large alkali feldspar crystals. Cumulitic textures with euhedral to subhedral feldspars are common; igneous layering occurs, however, owing to the presence of layers enriched in amphibole, clinopyroxene and plagioclase relics and others enriched in alkali feldspars and nepheline, although the latter mineral grows as an interstitial phase in the unlaminated syenites. Biotite is frequently present near the contact with basement rocks.

Nepheline-bearing alkali syenites are generally characterized by cumulitic textures and coarse grain size. The dominant phase is perthitic alkali

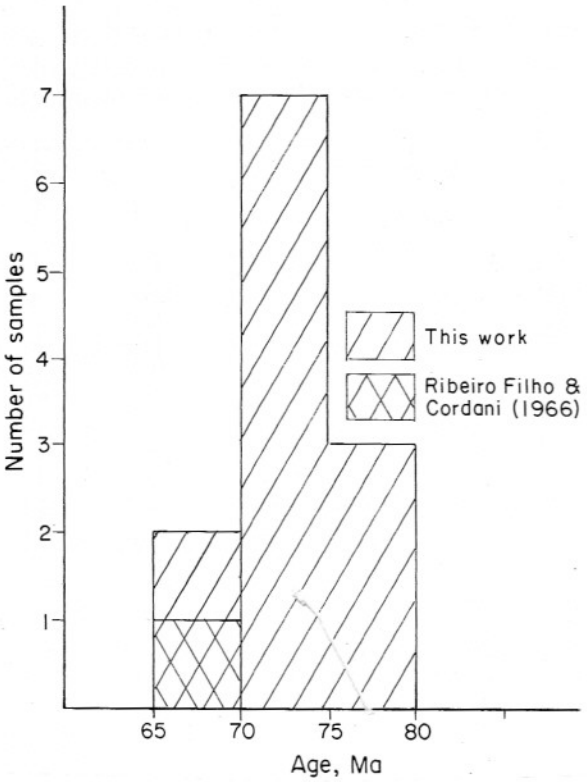

Figure 2 — Histogram for K/Ar values obtained on Morro Redondo samples; age reported by Ribeiro Filho & Cordani (1956) has been recalculated using new constants (Steiger & Jaeger, 1977).

feldspar with euhedral to subhedral habitus, enclosing plagioclase relics. Nepheline is always interstitial. The most common femic mineral is pargasitic amphibole, with kaersutitic cores and sporadic clinopyroxene relics; apatite, sphene and magnetite are again phases of early crystallisation.

Nepheline syenites, usually coarse-grained rocks, may be divided into two groups based on mineralogic and textural features. The first group (14, 13, 16, 18) shows pargasitic amphibole and interstitial nepheline as well as dominant

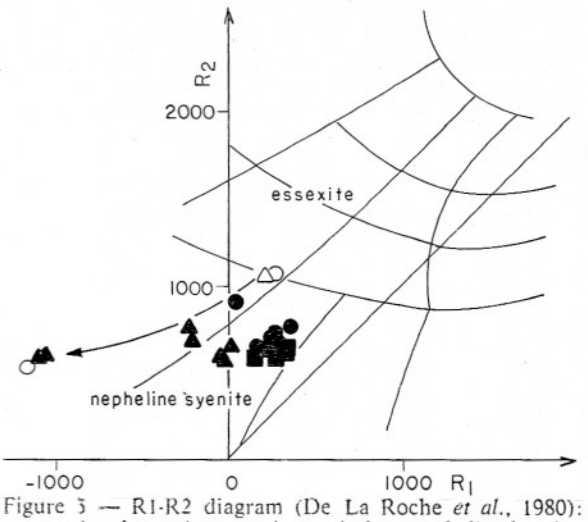

Figure 3 — R1-R2 diagram (De La Roche *et al.*, 1980): open triangles, microessexites; circles, nepheline-bearing syenites; squares, alkali syenites; triangles, nepheline syenites; open circles, phonotephritic and peralkaline phonolitic dykes. Arrow indicates the probable liquid line of descent.

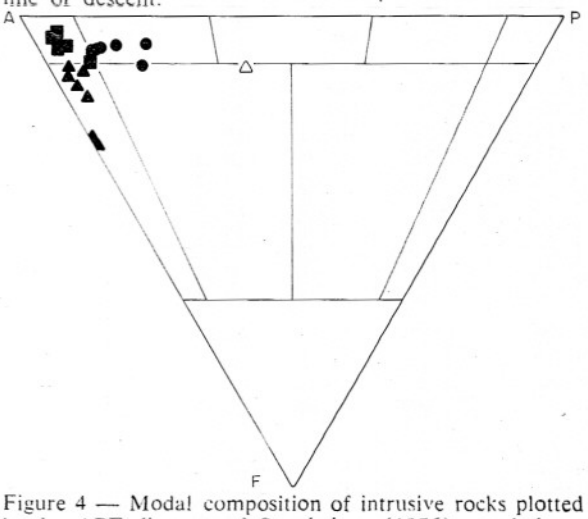

Figure 4 — Modal composition of intrusive rocks plotted in the APF diagram of Streckeisen (1976); symbols as in Fig. 3.

Table 1 — K-Ar ages of rocks from Morro Redondo. Mineral concentrates: Bi, biotite; Am, amphibole; WR, whole rock.

	%K	^{40}Ar rad (x10^6) (cm^3 S.T.P./g)	%Ar atm	Age ± 2 δ (Ma)
Phonotephrites				
2 (WR)	4.3296	11.65	56.78	68.0 ± 4.9
Syenites				
3 (Am)	2.0622	6.30	19.47	77.0 ± 2.6
4 (Bi)	7.3323	20.69	63.42	71.2 ± 5.0
6 (Bi)	6.7036	20.07	30 83	75.5 ± 4.2
15 (Am)	1.8488	5.86	30.56	79.8 ± 3.4
20 (Am)	2.2501	6.45	16.03	72.4 ± 3.4
23 (Bi)	7.4101	21.12	33 04	71.9 ± 2.5
27 (Bi)	7.3201	21.43	22.34	73.9 ± 3.2
Alkali syenites				
11 (Am)	1.6429	4.73	11.62	72.6 ± 2.9
Phonolites				
7 (WR)	5.8619	17.41	20.06	74.9 ± 3.2
Nepheline syenites				
26 (WR)	6.6434	18.98	11.20	72.1 ± 2.9

Table 2 — Major (wt %) and trace element (ppm) contents, CIPW norms ($Fe_2O_3/FeO = 0.15$) and modal analyses of the main rock types from Morro Redondo. E, microessexites; Pt, phonotephrites; S, nepheline-bearing syenites; NS, nepheline syenites; AS, alkali syenites; PP, peralkaline phonolites. D.I.* = Or + Ab + Ne + Ac + Ns.

	22 E	2 PT	15 S	20 S	27 S	5 S	4 S	3 S	23 S	14 NS	10 AS
SiO_2	52.26	51.36	54.24	58.19	57.85	58.70	58.70	59.14	58.75	57.37	59.26
TiO_2	2.44	2.23	1.91	1.37	1.52	1.23	1.23	1.21	1.07	1.00	0.97
Al_2O_3	17.93	17.90	17.45	18.45	18.13	18.26	18.41	18.45	18.23	19.70	19.02
Fe_2O_3	1.24	2.26	2.26	1.35	1.11	1.33	0.98	1.06	0.61	1.64	0.77
FeO	5.65	4.34	4.14	3.05	3.59	2.59	3.10	2.39	3.28	1.64	2.60
MnO	0.22	0.19	0.32	0.20	0.22	0.20	0.19	0.16	0.19	0.16	0.17
MgO	2.22	2.40	1.54	1.05	0.90	0.90	0.90	0.69	0.67	0.64	0.63
CaO	5.90	5.81	4.84	3.52	3.16	2.73	2.76	2.92	2.59	3.26	2.52
Na_2O	4.88	6.26	5.13	5.04	4.11	4.22	4.51	4.51	4.68	6.61	5.12
K_2O	5.57	5.18	6.64	6.82	8.37	8.43	8.08	8.41	8.35	6.90	7.64
P_2O_5	0.94	0.98	0.70	0.36	0.26	0.24	0.25	0.24	0.24	0.29	0.21
LO I	0.74	1.09	0.82	0.60	0.77	0.82	0.88	0.81	1.34	0.79	1.09
Total	99.99	100.00	99.99	100.00	99.99	100.01	99.99	99.99	100.00	100.00	100.00
V	100	160	93	38	33	28	26	32	25	42	25
Rb	110	125	158	115	113	116	116	112	126	126	129
Sr	3387	1784	1964	3817	2415	2517	3141	3607	1299	3581	3396
Ba	1908	1653	1219	1928	842	1407	2031	1951	379	2332	1713
Zr	463	573	684	362	382	263	372	329	338	594	453
Nb	125	150	370	96	108	83	92	107	117	191	125
Y	38	32	68	30	24	21	23	29	27	23	20
La	148	114	306	104	96	83	74	82	102	132	106
Ce	290	212	187	218	192	165	157	165	180	247	208
Nd	118.05	82.26	187.21				70.75	76.61			
Sm	20.38	12.39	28.59				10.55	11.75			
Eu	6.59	3.24	7.21				6.40	8.77			
Gd	14.75	8.76	20.36				7.42	8.32			
Dy	9.46	6.53	14.86				5.40	6.21			
Er	4.04	2.93	7.13				2.31	2.70			
Yb	3.21	2.55	6.35				1.75	2.06			
Lu	0.41	0.31	0.73				0.21	0.24			
Or	32.88	30.57	39.18	40.25	49.40	49.76	47.69	49.64	49.28	40.73	45.09
Ab	21.14	18.16	20.42	32.25	23.71	26.20	27.93	26.57	26.46	25.92	31.61
An	10.56	5.44	4.97	7.57	6.30	5.98	6.12	5.26	4.07	3.70	6 35
Ne	10.09	18.84	12.44	5.62	5.98	5.14	5.53	6.27	7.10	16.24	6.33
Ns											
Ac											
Wo											
Wo-Di	5.24	7.08	6.03	3.14	3.20	2.50	2.47	3.19	3 01	4.41	1.99
En-Di	2.37	3.39	2.22	1.17	1.05	0.84	0.86	1.11	0.87	1.46	0.62
Fs-Di	2.83	3.58	3.93	2.04	2.26	1.73	1.68	2.17	2.28	3.09	1.45
Fo	2.20	1.79	1.12	1.01	0.83	0.97	0.96	0.42	0.56	0.09	0.66
Fa	2.30	2.09	2.19	1.94	1.98	2.22	2.05	0.91	0 61	0.20	1.72
Mt	1.30	1.22	1.19	0.74	0.82	0.88	0.80	0.76	0.64	0.60	0.63
Il	4.64	4.24	3.63	2.61	2.89	2.34	2.34	2.30	2.04	1.90	1 85
Ap	2.23	2.32	1.66	0.85	0.62	0.57	0.59	0.57	0.57	0.69	0.50
DI*	64.92	67.58	72.05	78.12	19.10	81.09	81.15	82.47	82.85	82.88	83.03
Af	36.0		49.9	58.2	63.3	63.5	64 0	63.2	62.8	65.2	71.7
Pl	24.1		12.0	16.4	12.5	9.5	8.6	8.3	7.6	2.5	6.4
Ne	6.9		7.3	4.5	4.2	5.2	5.0	5.7	5.8	14.3	5.1
Am	13 6		24.0	15.6	11.3	13.5	13.8	14.6	14.1	12.5	12.9
Bi	6.3		0.7	1.3	3.4	2.2	2 0	1.8	4.3		
Py	7.7		1.3	1.6	2.0	0.7	1.1	1.0	0.7	0.2	
Sp	1.3		2.6	0.9	1.5	3.5	3.1	3.3	3.2	3.2	2.9
Op	3.0		0.7	1.1	1.4	0.4	1.8	1.6	1.2	2.4	1.5
Ap	1.1		1.5	0.4	0.4	0.5	0.5	0.4	0.4	2.5	0.5

euhedral alkali feldspar; paragenesis is completed by relic plagioclases and clinopyroxene, apatite, sphene and magnetite. The second group differs due to the higher abundances of nepheline (25-26% by volume), often in subhedral grains, and the presence of hastingsitic amphibole and Fe-salitic clinopyroxene; the early phases apatite, sphene and magnetite are still present.

Phonotephrites are weakly porphyritic with an assemblage consisting of alkali feldspar, biotite, amphibole, Ti-salite, nepheline and nosean, sphene, apatite and Ti-magnetite, each of them present in the groundmass with the exception of amphibole.

Table 2 (cont.)

	9 AS	12 AS	13 NS	16 NS	11 AS	28 AS	8 NS	1 NS	18 NS	7 P	26 NS
SiO_2	59.93	59.97	59.45	58.80	60.31	60.92	60.42	56.03	60.91	58.00	57.31
TiO_2	1.08	1.11	0.68	0.79	0.81	0.81	0.70	0.52	0.40	0.26	0.33
Al_2O_3	18.25	18.03	20.05	19.89	18.84	18.66	18.96	21.92	19.70	20.71	21.80
Fe_2O_3	1.01	0.79	0.72	1.10	0.75	1.08	1.01	0.83	0.55	1.37	0.58
FeO	2.54	2.89	1.57	1.62	2.15	1.75	1.79	1.26	1.19	0.99	1.30
MnO	0.19	0.18	0.11	0.15	0.16	0.14	0.20	0.14	0.11	0.21	0.11
MgO	0.67	0.65	0.34	0.40	046	0.40	0.34	0.22	0.15	0.04	0.08
CaO	2.64	2.52	2.50	2.77	2.04	2.11	2.07	1.85	1.68	1.37	1.41
Na_2O	4.23	4.17	6.02	6.73	5.46	4.64	6.08	8.98	5.61	9.49	8.68
K_2O	8.63	8.78	7.36	7.01	7.83	8.73	7.82	6.71	8.79	6.92	7.61
P_2O_5	0.19	0.15	0.17	0.19	0.17	0.11	0.11	0.06	0.05	0.02	0.03
LO I	0.65	0.75	1.03	0.54	1.01	0.65	0.51	1.57	0.84	0.62	0.75
Total	100.01	99.99	100.00	99.99	99.99	100.00	100.01	100.09	99.99	100.00	99.99
V	25	21	27	29	17	23	18	16	14	8	9
Rb	110	115	134	145	129	123	161	131	127	245	160
Sr	1749	1078	3643	3141	2214	2192	892	372	287	75	445
Ba	871	190	2411	1943	1100	983	297	79	80	45	95
Zr	292	395	535	773	612	314	657	475	353	1288	568
Nb	126	154	139	198	132	95	209	216	143	229	123
Y	27	29	9	40	21	20	41	23	11	29	14
La	104	102	90	169	93	92	139	110	116	198	87
Ce	225	217	177	287	199	163	224	171	181	23	135
Nd				82.69	85.20			95.75			28.24
Sm				13.07	12.76			4.63			3.66
Eu				4.26	5.41			1.19			1.50
Gd				9.36	8.74			3.42			2.70
Dy				6.73	6.78			2.65			2.09
Er				3.48	3.14			1.73			1.37
Yb				3.38	2.68			2.99			1.57
Lu				0.46	0.32			0.28			0.22
Or	50.94	51.82	43.44	41.38	46.22	51.53	46.16	39.60	51.88	40.84	44.92
Ab	28.19	27.65	31.63	29.61	33.49	30.32	31.54	20.51	28.20	24.42	19.05
An	5.32	4.54	5.95	3.36	3.77	4.30	1.35		2.64		
Ne	4.10	4.12	10.44	14.79	6.87	4.83	10.76	29.71	10.42	23.58	27.46
Ns										2.64	0.67
Ac								0.52		0.85	0.70
Wo				0.10				0.76			0.31
Wo-Di	2.72	2.91	2.23	3.71	2.18	2.27	3.42	2.90	2.24	2.78	2.52
En-Di	0.86	0.88	0.60	0.99	0.60	0.59	0.75	0.55	0.37	0.09	0.20
Fs-Di	1.96	2.15	1.74	2.91	1.69	1.80	2.91	2.58	2.06	3.05	2.61
Fo	0.56	0.51	0.17		0.38	0.28	0.07				
Fa	1.40	1.38	0.53		1.18	0.95	0.29		0.02	0.39	
Mt	0.66	0.69	0.43	0.50	0.54	0.52	0.52	0.12	0.32		
Il	2.05	2.11	1.29	1.50	1.54	1.54	1.33	0.99	0.76	0.49	0.63
Ap	0.45	0.36	0.40	0.45	0.40	0.26	0.26	0.14	0.12	0.05	0.07
DI*	83.23	83.60	83.51	85.57	86.57	86.68	88.46	90.34	90.50	92.34	92.79
Af	76.7	78.2	67.0	66.8	78.5	75.7	74.0	69.0	65.0		70.7
Pl	3.4	3.6	4.5	2.5	3 6	7.9	2.4		3.6		
Ne	3.9	4.3	10.2	13.0	6.2	8.2	10.5	26.5	11.1		25.5
Am	11.1	10.2	13.3	12.5	8.8	5.6	8.8	2.4	5.8		2.4
Bi											
Py	0.7	0.1		0.4	0.7			0.4	0.3		0.1
Sp	2.7	2.8	2.2	2.4	1.2	1.1	2.0	1.4	2.7		1.0
Op	1.3	0.7	2.4	2.0	0.6	1.3	2.1	0.6	1.4		0.3
Ap	0.3	0.2	0.4	0.4	0.4	0.2	0.2	0.1	0.1		0.1

Peralkaline phonolites range from subaphyric to weakly porphyritic types, with alkali feldspar and hastingsitic amphibole as phenocrysts in a nepheline-rich groundmass.

BULK-ROCK CHEMISTRY

XRF and ICP analyses were carried out for major, minor and trace elements on 22 representative rocks (Table 2).

In the TAS diagram (Fig. 5) the samples fall above the curve separating the strongly alkaline rocks from the alkaline ones (Saggerson & Williams, 1964). On the basis of the K_2O/Na_2O ratio, the rocks may be divided into two groups: one with a ratio of 0.9-1.0 and the other with a ratio of about 2. Both groups exhibit a clear potassic affinity as also seen in the CaO — K_2O — Na_2O diagram (Fig. 6) which also shows

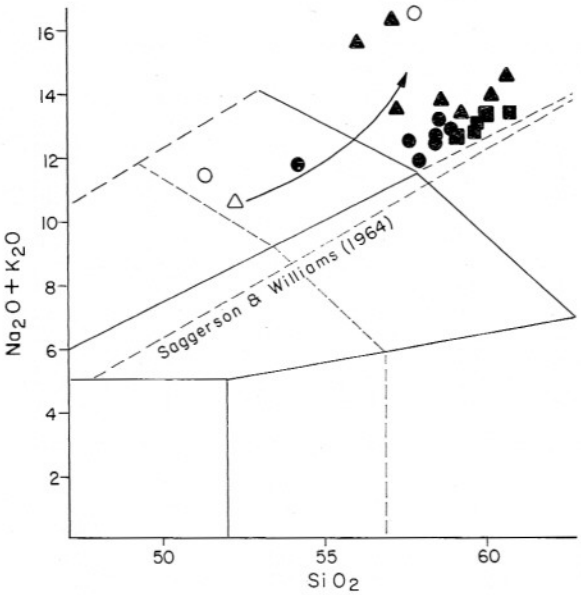

Figure 5 — TAS diagram (Le Bas *et al.*, 1986); symbols as in Fig. 3. Arrow indicates the probable liquid line of descent.

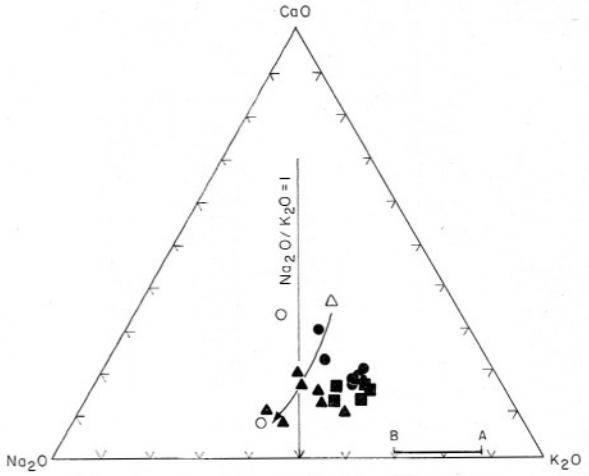

Figure 6 — CaO-Na_2O-K_2O diagram for Morro Redondo samples; the arrow denotes the probable liquid line of descent; A-B indicates alkali feldspar compositions; symbols as in Fig. 3.

the alkali feldspar compositional range. The position and spreading of the rocks in the diagram, together with textural evidence, point to alkali feldspar cumulus processes for some of the samples.

The most evolved nepheline syenites and phonolites display a mild peralkaline character (1.01-1.12), as indicated by the presence of Na-metasilicate and acmite in their CIPW norms.

The least to the most evolved samples (22

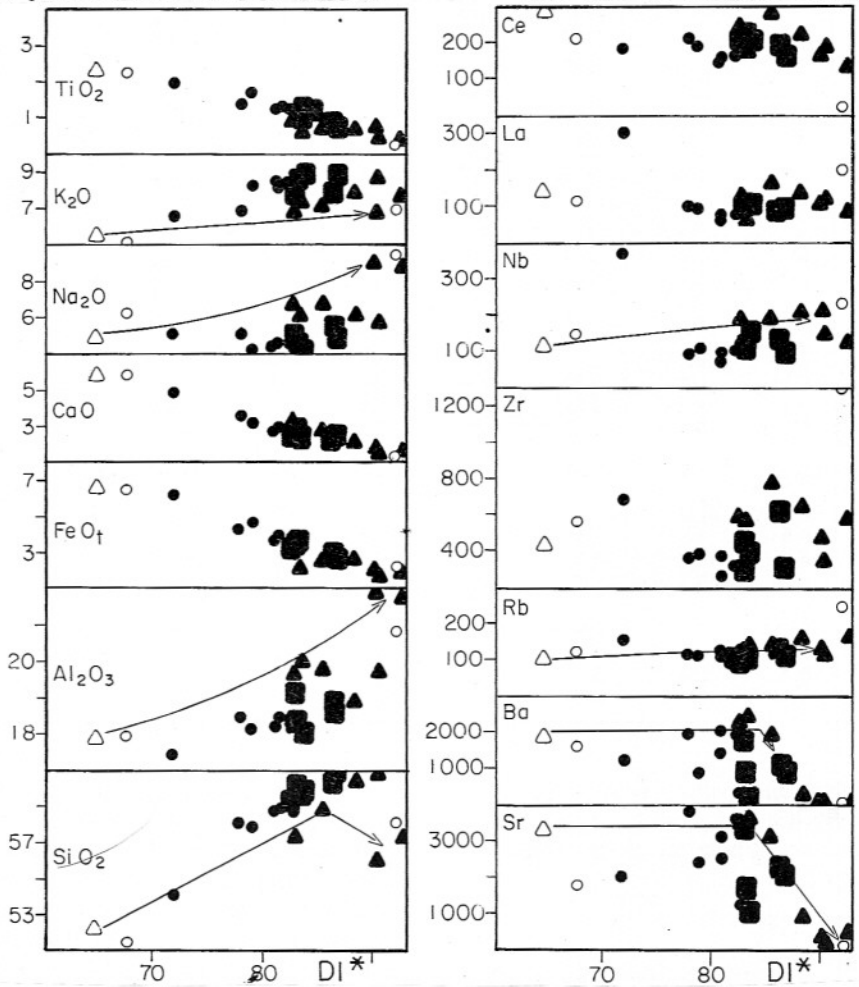

Figure 7 — Variation diagrams (D.I* vs major and trace elements; D.I.*=Ab+Or+Ne+Ac+Ns) and probable liquid line of descent (solid line) for Morro Redondo rocks; symbols as in Fig. 3.

to 1-26) reveal a general decrease in TiO_2, CaO, FeO_t, and an increase, although more scattered, in SiO_2, Al_2O_3, Na_2O and K_2O (Table 2, Fig. 7).

Lower values in Na_2O and Al_2O_3 are usually associated with higher values in SiO_2 and K_2O, with smooth trends in FeO_t, testifying that alkali feldspar is preferentially involved in cumulus processes.

As regards trace elements, V diminishes and Rb, Zr and Nb increase throughout the suite,

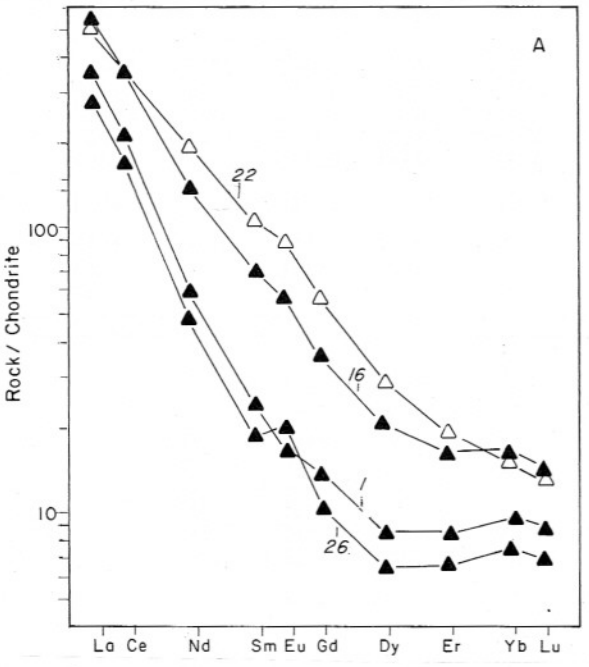

Figure 8a — Chondrite-normalized values for REE of Morro Redondo rocks (chondrite values from Boynton, 1984); symbols as in Fig. 3.

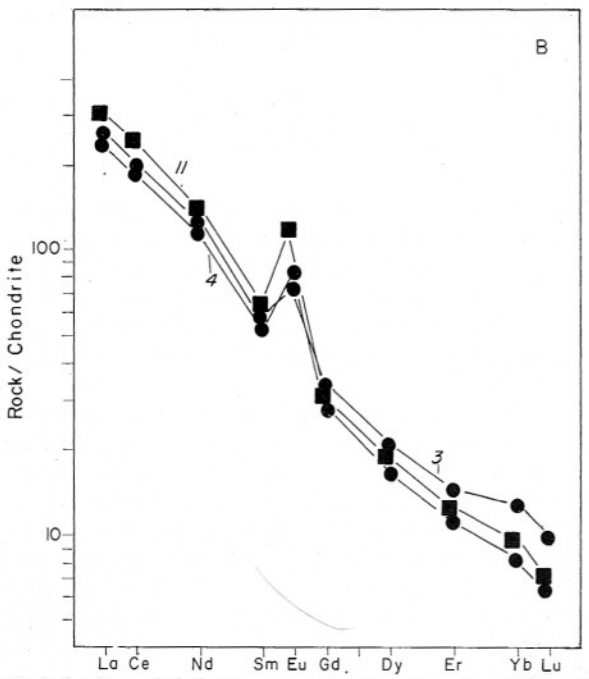

Figure 8b — Chondrite-normalized values for REE of Morro Redondo rocks (chondrite values from Boynton, 1984); symbols as in Fig. 3.

while Sr and Ba increase to less evolved nepheline syenites, and then abruptly decrease. The scattering of the data observed for Sr, Ba, Zr, Nb and Y is probably due to the inhomogeneous distribution and cumulus of alkali feldspar and sphene, as well as variations in concentration of these elements in the host minerals.

The REE show three distinct chondrite-normalized patterns in the analysed rocks of the complex. The first (represented by less evolved rocks: 2, 22) is nearly linear and positively fractionated from La to Lu, with very small positive Eu anomalies (Fig. 8a). The second pattern is represented by some of the samples which show cumulus evidence (3, 4, 11), with strong positive Eu anomalies ($Eu/Eu^* = 1.48 - 2.6$) (Fig. 8b). The third is concave upwards and occurs in the most evolved rocks (1, 26) and, less evidently, in 16, owing to apatite and sphene fractionation that preferentially remove MREE. Some samples of this group also show positive Eu anomalies (Fig. 8a).

MINERAL CHEMISTRY

Feldspars

In the fine-grained essexites (22) plagioclase is an early product of crystallisation with content in anorthite molecule ranging from 40% (core) to 30.6% (rim). In the other rocks where it occurs, plagioclase is rarely euhedral but more appears often as corroded cores in alkali feldspar, with oscillatory zoning from $An_{39.2}$ to An_{14}.

Phono-tephritic rocks completely lack plagioclase phenocrysts.

Plagioclase-rock geothermometers (Kudo-Weill, 1970; Mathez, 1973) for sample 22 indicate equilibrium temperatures slightly above 1000°C (1063-1013°C) for cores of crystals; these values should probably be considered as maximum temperatures, owing to the chemical zonation of the crystals.

Alkali feldspar is by far the most dominant phase in the rocks of the complex and occurs as granular or large tabular Carlsbad-twinned crystals: it is frequently perthitic and cryptoperthitic, seldom coarsely unmixed, and sometimes crossed by thin veins of secondary albite.

The host composition of alkali feldspar obtained by systematic analysis of exsolved regions (Table 3) does not allow chemical discrimination among the different lithotypes. However, a slight increase in Ab content going from microessexites to evolved nepheline syenites (Or_{70-63}) may be observed. High Or contents (Or_{79}) were also observed in the most evolved nepheline syenites (26). These feldspar compositions are far from the low temperature termination of the plagioclase-alkali feldspar field boundary and the thermal minimum of the Ab-Or diagram, suggesting relatively high crystallisation temperatures and/or equilibrations with potassic liquids.

Table 3 — Microprobe composition of representative feldspars from Morro Redondo (*c* and *r*, respectively, core and rim of crystals).

	22 Ac	22 Ar	20 Ac	4 Ac	4 Ar	3 Ac	3 Ar	11 Ac	11 Ar	11 Br
SiO_2	57.59	60.49	69.19	58.81	60.88	58.53	61.17	58.35	60.73	64.81
Al_2O_3	26.56	24.85	24.71	25.99	24.40	26.07	24.43	26.24	24.80	21.84
Fe_2O_3	0.17	0.08	0.18	0.07	0.15	0.14	0.18	0.19	0.10	0.09
CaO	8.39	6.16	6.39	7.61	5.67	7.75	5.75	7.93	6.13	2.82
Na_2O	6.73	8.04	7.83	7.24	8.28	7.14	8.27	6.97	8.03	9.80
K_2O	0.17	0.21	0.27	0.14	0.24	0.14	0.26	0.26	0.28	0.49
Total	99.61	99.83	99.57	99.86	99.62	99.71	100.06	99.94	100.07	99.85
Si	10.3553	10.7818	10.7665	10.5187	10.8632	10.4889	10.8690	10.4463	10.7989	11.4471
Al	5.6283	5.2199	5.2090	5.4783	5.1310	5.5037	5.1157	5.5363	5.1971	4.5461
Fe^{3+}	0.0256	0.0119	0.0269	0.0105	0.0224	0.0210	0.0267	0.0284	0.0149	0.0133
Ca	1.6162	1.1763	1.2245	1.4582	1.0839	1.4873	1.0946	1.5210	1.1678	0.5336
Na	2.3458	2 7770	2.7153	2.5106	2.8643	2.4799	2.8488	2.4192	2.7696	3.3557
K	0.0390	0.0477	0.0616	0.0319	0.0546	0.0320	0.0589	0.0594	0.0635	0.1104
Total	20.0102	20.0146	20.0040	20.0082	20.0195	20.0088	20.0137	20.0106	20.0117	20.0063
Ab wt%	57.19	68.14	66.55	61.36	70.34	60.61	69.95	59.06	67.95	83.08
An wt%	41.80	30.62	31.84	37.81	28.24	38.56	28.51	39.40	30.40	14.02
Or wt%	1.01	1.24	1.60	0.83	1.42	0.83	1.54	1.54	1.65	2.90

	22 A	20 A	4 A	3 A	14 A	11 A	1 A	26 Ac	26 A
SiO_2	65.05	65.49	65.47	65.56	65.44	65.50	65.80	64.84	64.97
Al_2O_3	19.17	19.06	18.83	18.87	18.83	19.02	18.82	18.85	18.78
Fe_2O_3	0.09	0.10	0.06	0.08	0.06	0.07	0.04	0.09	0.23
CaO	0.60	0.45	0.17	0.24	0.23	0.20	0.13	0 21	0.23
Na_2O	3.27	3.68	3.35	3.76	3.61	3.92	4.23	1.97	2.30
K_2O	11.71	11.27	11.94	11.29	11.50	11.10	10.71	13.89	13.40
Total	99.89	100.05	99.82	99.80	99.67	99.81	99.73	99.85	99.91
Si	11.8690	11.9046	11.9477	11.9414	11.9442	11.9221	11.9643	11.9172	11.9176
Al	4.1221	4.0831	4.0497	4.0506	4.0504	4.0799	4.0329	4.0829	4.0598
Fe^{3+}	0.0137	0.0152	0.0092	0 0122	0.0092	0.0107	0.0061	0 0138	0.0353
Ca	0.1173	0.0876	0.0332	0.0468	0.0450	0.0390	0.0253	0.0413	0.0452
Na	1.1567	1.2982	1.1865	1.3292	1.2774	1.3848	1.4911	0.7019	0.8184
K	2.7254	2.6132	2.7794	2.6231	2.6774	2.5772	2.4841	3.2564	3.1354
Total	20.0042	20.0019	20.0058	20.0034	20.0035	20.0136	20.0038	20.0136	20.0117
Ab wt%	27.71	31.17	28.44	31.93	30.65	33.28	35.89	16.70	19.51
An wt%	2.98	2.23	0.85	1.19	1.15	0 99	0.65	1.04	1.14
Or wt%	69.31	66.60	70.71	66.88	68.20	65.73	63.46	82.25	79.34

The BaO content of alkali feldspars, obtained by semiquantitative microprobe analysis, is low and decreases towards nepheline syenites (from 0.4% to nearly zero).

Temperatures obtained with two-feldspar geothermometers (Stormer, 1975; Ghiorso, 1984) are in the range 780-980°C, and thus in acceptable agreement with temperatures estimated for liquids in the petrogeny residua's system at $P_{H20} = 1$ kbar (see below).

Nepheline

It is the dominant feldspathoid in the intrusive rocks and occurs as poikilitic intercumulus crystals; only in the most evolved nepheline syenites does nepheline show a tendency toward euhedral habitus, reaching perhaps cotectic crystallisation with alkali feldspar.

There are very few compositional variations, and the nephelines tend to cluster around Ne_{75}-Ks_{20} Qz_5 in the Ne-Ks-SiO_2 diagram, well within the field for natural plutonic nephelines (Dollase & Thomas, 1978) and close to the natural nepheline composition plane of Barth (1963) (Table 4, Fig. 9).

The CaO content is high, not very common for plutonic nephelines, suggesting appreciable solid solutions towards anorthite. Ca-rich cores with less Ca-rich rims were found associated in nephelines of relatively high temperature (Henderson & Gibb, 1983). Taking into account nepheline solid solution limits as defined by Hamilton (1961), silica excess indicates equilibration and/or reequilibration temperatures higher than 700°C, followed by rapid cooling.

Nosean is the most widespread feldspathoid in the effusive rocks of the complex.

Table 4 — Microprobe composition of representative nephelines from Morro Redondo.

	2 A	20 A	3 A	14 A	14 B	1 A	26 A	26 B
SiO_2	43.94	43.99	43.40	43.80	43.66	44.26	43.99	43.75
Al_2O_3	33.72	33.56	34.04	33.77	33.67	33.50	33.39	33.65
Fe_2O_3	0.35	0.34	0.17	0.24	0.37	0.25	0.33	0.26
CaO	1.17	1.54	1.63	1.23	1.40	1.21	1.19	1.26
Na_2O	15.58	15.25	15.13	15.55	15.30	15.42	15.46	15.32
K_2O	5.29	5.09	5.51	5.32	5.34	5.22	5.35	5.72
Total	100.05	99.77	99.98	99.91	99.74	99.86	99.71	99.96
Si	8.3866	8.4085	8.3105	8.3737	8.3639	8.4493	8.4246	8.3752
Al	7.5848	7.5599	7.6817	7.6086	7.6015	7.5367	7.5360	7.5916
Fe^{3+}	0.0559	0.0543	0.0272	0.0384	0.0593	0.0399	0.0528	0.0416
Ca	0.2392	0.3154	0.3344	0.2519	0.2873	0.2475	0.2442	0.2584
Na	5.7650	5.6512	5.6167	5.7634	5.6823	5.7069	5.7400	5.6857
K	1.2879	1.2411	1.3459	1.2974	1.3049	1.2711	1.3069	1.3968
Total	23.3195	23.2305	23.3164	23.3333	23.2993	23.2514	23.3045	23.3494
Qz	5.90	6.15	6.10	6.10	6.00	6.00	5.90	6.25
Ne	71.51	69.90	69.45	71.28	70.13	70.78	70.86	70.22
Ks	17.96	17.09	18.50	17.86	17.93	17.52	17.96	19.20
An	4.67	5.26	4.73	4.22	4.80	5.10	4.68	4.04

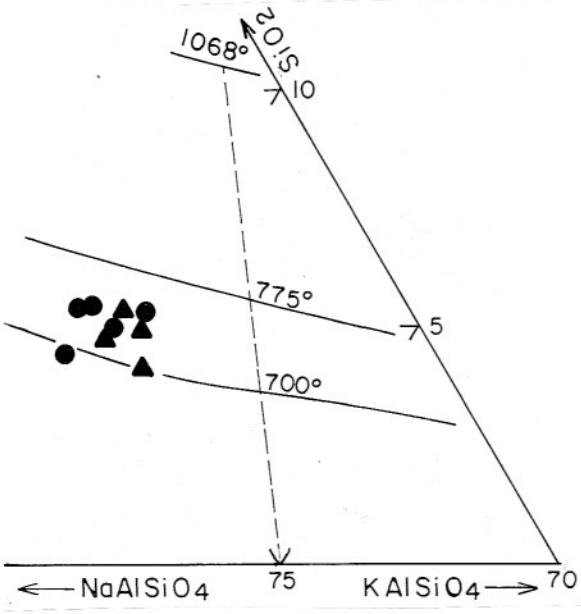

Figure 9 — Nepheline compositions in the Ne-Ks-SiO_2 diagram. Solid lines denote solid solution limits at different temperatures (after Hamilton, 1961). Dashed line indicates nepheline composition plane of Barth (1963).

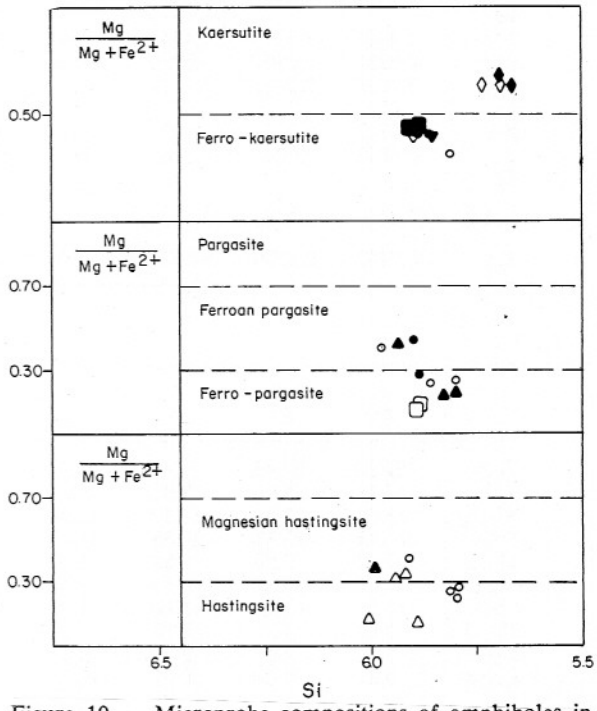

Figure 10 — Microprobe compositions of amphiboles in the nomenclature diagram of Leake (1978) for Morro Redondo rocks. Symbols: as in Fig. 3, except for microessexites (inverted triangles) and phonotephrites (lozenges); open symbols represent crystal rims or late crystallization phases.

Amphiboles

Alkali-calcic amphiboles are the dominant femic phase throughout the suite, excluding microessexites, and are present as continuously zoned crystals from yellow-brown kaersutitic cores through green Fe-pargasitic mantles to hastingsitic rims (Table 5, Fig. 10). All the amphiboles possess more than 0.25 K atoms per half cell unit and are therefore termed potassian (Leake, 1978); this is in agreement with the potassic affinity of the host rocks. There is a clear increase in Fe^{2+}, Fe^{3+} and Al, and a decrease in Ti, Mg and, less evidently, Na and K, from microessexites to nepheline syenites (Fig. 11). General trends suggest that, besides normal substitution mechanisms such as $Mg = Fe^{2+}$, others like $Fe^{2+} + Si = Fe^{3+} + Al^{IV}$ and $Ti + O = Fe^{3+} + OH$, indicating P_{H2O} increase, may operate in modifying amphibole chemistry (see Bedard, 1988). The slight decrease in Na and K is probably due to competing alkali-rich phases like feldspars and nepheline and to the entry of OH ions in the lattice structure.

Clinopyroxenes

Excluding microessexites, Ca-rich pyroxene

Table 5 — Microprobe composition of representative amphiboles from Morro Redondo. Structural formulae calculated on the basis of 23 atoms of O. FeO* and Fe_2O_3* according to Papike *et al.* (1974). Mg = Mg/Mg + Fe^{3+} + Fe^{2+}.

	2 Ac	2 Ar	2 Bc	2 Br	22 Ac	22 Ar	20 Ac	20 Ar	20 Br	4 Ac
SiO_2	37.69	37.67	37.96	37.90	37.45	37.74	38.29	38.58	38.24	37.72
TiO_2	6.68	6.45	6.52	6.32	5.23	4.66	3.88	2.69	2.70	4.74
Al_2O_3	13.22	13.06	13.09	12.82	11.75	12.26	12.52	12.64	12.87	11.89
FeO_t	11.79	12.27	11.51	12.26	19.14	18.96	18.52	19.67	19.88	18.95
MnO	0.20	0.24	0.22	0.28	0.69	0 68	1.11	1.26	1.24	0.90
MgO	12.19	11.92	12.39	11.83	7.54	7.50	8.31	7.65	7.69	7.63
CaO	11.89	11.97	11.95	11.82	11.28	11.35	11.16	11.23	11.16	11.57
Na_2O	2.19	2.07	2.07	2.12	2.40	2.42	2.35	2.30	2.34	2.22
K_2O	2.00	2.08	2.07	2.03	1.99	1.96	2.00	1.90	2.00	2.07
Cr_2O_3					0.02	0.01	0.01	0.01	0.01	0.01
Total	97.85	97.73	97.78	97.38	97.49	97.54	97.95	97.93	98.13	97.70
Fe_2O_3*							1.31	1.87	2.37	
FeO*	11.79	12.27	11.51	12.26	19.14	18.96	17.14	17.99	17.75	18.95
Total*	97.85	97.73	97.78	97.38	97.49	97.54	98.08	98.12	98.37	97.70
Si	5 6611	5.6809	5.6963	5.7311	5.8568	5.8834	5.9024	5.9691	5.9095	5.8839
Ti	0.7545	0.7314	0.7357	0.7186	0.6150	0.5463	0.4497	0.3130	0.3137	0.5560
Al	2.3401	2.3211	2.3149	2.2846	2.1656	2.2524	2.2745	2.3048	2.3439	2.1858
Fe^{3+}							0.1517	0.2180	0.2758	
Fe^{2+}	1.4808	1.5473	1.4443	1.5502	2.5030	2.4716	2.2097	2.3269	2.2932	2.4718
Mn	0.0254	0 0307	0.0280	0.0359	0.0914	0.0898	0.1449	0.1651	0.1623	0.1189
Mg	2.7289	2.6793	2.7711	2.6662	1.7575	1.7426	1.9092	1.7641	1.7712	1.7739
Ca	1.9133	1.9339	1.9211	1.9149	1.8899	1.8956	1.8430	1.8614	1.8477	1.9335
Na	0.6377	0.6052	0.6022	0.6215	0.7277	0.7314	0.7023	0.6899	0.7011	0.6714
K	0.3832	0.4001	0.3962	0.3916	0.3970	0.3898	0.3933	0 3750	0.3943	0.4119
Cr					0.0025	0.0012	0.0012	0.0012	0.0012	0.0012
Total	15.9249	15.9298	15.9098	15.9145	16.0064	16.0041	15.9819	15.9884	16.0139	16.0082
Mg	0.6482	0.6339	0.6574	0.6323	0.4125	0.4135	0.4471	0.4094	0.4081	0.4178

	4 Ar	4 Bc	4 Br	3 Ac	3 Ar	3 Br	3 Cc	3 Cr	14 Ac	14 Ar
SiO_2	36.98	37.46	36.40	36.84	36.80	36.83	37.28	36.68	38.49	37.78
TiO_2	2.74	4.94	2.91	5.09	2.25	2.40	3.92	3.04	2.51	2.53
Al_2O_3	13.00	11.97	13.10	12.08	13.46	13.60	12.46	13.39	11.96	12.46
FeO_t	24.13	18.79	24.35	21.29	23.77	23.43	22 32	23.78	21.41	22.24
MnO	1.42	0.99	1.59	1.20	1.54	1.46	1.32	1.38	1.49	1.53
MgO	4.51	7.57	4.13	5.87	4.75	4.99	5.18	4.46	6.89	6.12
CaO	11.14	11.49	11.12	11.29	11.15	11.09	11.44	11.09	11.09	11.05
Na_2O	2.18	2.27	2.10	2.24	2.14	2.14	2.14	1.99	2.30	2.25
K_2O	2.01	2.05	2 03	2.00	2.04	2.02	1.91	1.97	1.98	1.97
Cr_2O_3	0.01	0.01	0.01	0.01	0.01	0.03	0.03	0.02	0.01	0.01
Total	98.12	97.54	97.74	97.91	97.91	97.99	98.00	97.80	98.13	97.94
Fe_2O_3*	2.19		2.43		3.24	3.26	0 36	2.34	2.54	2.87
FeO*	22.16	18.79	22.16	21.29	20.86	20.50	21.99	21.67	19.12	19.66
Total*	98.34	97.54	97.98	97.91	98.23	98.32	98.04	98.03	98.38	98.23
Si	5.8525	5.8543	5.7991	5.8111	5.8136	5.7988	5 8848	5.8072	5.9948	5.9203
Ti	0.3261	0.5805	0.3486	0.6037	0.2673	0.2841	0.4653	0.3619	0.2940	0.2981
Al	2.4246	2.2046	2.4596	2.2456	2.5060	2.5235	2.3179	2.4983	2.1953	2.3011
Fe^{3+}	0.2612		0 2917		0.3851	0.3859	0 0432	0.2792	0.2979	0.3382
Fe^{2+}	2.9321	2.4555	2.9522	2.8081	2.7549	2.6988	2.9029	2.8689	2.4905	2.5760
Mn	0.1903	0.1310	0.2145	0.1603	0.2060	0.1947	0.1765	1.1850	0.1965	0.2031
Mg	1.0678	1.7633	0 9807	1.3800	1.1184	1.1710	1.2187	1.0524	1.5994	1.4294
Ca	1 8888	1.9237	1.8979	1.9079	1.8871	1.8706	1.9347	1.8810	1.8505	1.8551
Na	0.6689	0.6878	0.6486	0.6850	0.6554	0.6532	0.6549	0.6108	0 6945	0.6836
K	0.4058	0.4087	0 4125	0.4024	0.4111	0.4057	0 3846	0.3978	0.3934	0.3938
Cr	0.0013	0.0012	0.0013	0.0012	0.0012	0.0037	0.0037	0.0025	0.0012	0.0012
Total	16.0152	16.0105	16.0067	16.0055	16.0062	15.9900	15.9872	15.9452	16.0080	15.9999
Mg	0.2499	0.4180	0.2321	0.3295	0.2626	0.2752	0.2926	0.2505	0.3645	0.3291

Table 5 (cont.)

	11 Ac	11 Ar	11 Bc	11 Br	1 Ac	1 Ar	26 Ac	26 Ar	26 Bc	26 Br
SiO_2	37.90	36.61	37.96	36.63	38.15	37.71	36.30	37.43	36.41	36.43
TiO_2	5.09	2.90	5.08	2.87	3.30	1.90	3.67	1.66	3.43	2.14
Al_2O_3	11.80	12.81	11.80	12.77	12.60	12.10	13.02	11.91	13.05	11.96
FeO_t	17.82	26.57	18.15	26.15	18.17	22.45	24.69	27.07	24.96	28.34
MnO	1.04	1.97	1.09	2.01	1.63	2.31	1.52	2.29	1.70	2.32
MgO	8.21	2.17	8.07	2.47	7.77	5.72	3.50	2.35	3.22	1.98
CaO	11.32	10.91	11.40	10.87	12.01	11.59	10.98	10.73	11.04	10.75
Na_2O	2.50	2.19	2.48	2.20	2.19	2.22	2.15	2.17	2.15	2.12
K_2O	1.93	1.90	1.91	1.90	1.80	1.81	2.04	1.93	2.02	1.98
Cr_2O_3	0.01	0.02	0.01	0.02	0.01	0.05	0.02	0.01	0.01	0.01
Total	97.62	98.05	97.95	97.89	97.63	97.86	97.89	97.55	97.99	98.03
Fe_2O_3*		1.26		1.42		3.61	1.13	2.41	1.06	3.98
FeO*	17.82	25.44	18.15	24.87	18.17	19.20	23.67	24.91	24.01	24.76
Total*	97.62	98.18	97.95	98.03	97.63	98.22	98.00	97.79	98.10	98.43
Si	5.8838	5.8938	5.8835	5.8937	5.9351	5.9381	5.8027	6.0526	5.8249	5.8932
Ti	0.5943	0.3511	0.5920	0.3472	0.3860	0.2250	0.4411	0.2018	0.4126	0.2603
Al	2.1593	2.4304	2.1554	2.4214	2.3101	2.2455	2.4528	2.2697	2.4604	2.2801
Fe^{3+}		0.1527		0.1721	0.0002	0.4275	0.1359	0.2927	0.1270	0.4844
Fe^{2+}	2.3137	3.4241	2.3523	3.3462	2.3635	2.5286	3.1644	3.3676	3.2120	3.3492
Mn	0.1368	0.2686	0.1431	0.2739	0.2148	0.3081	0.2058	0.3136	0.2303	0.3179
Mg	1.9000	0.5207	1.8642	0.5923	1.8016	1.3425	0.8339	0.5664	0.7678	0.4774
Ca	1 8831	1.8817	1.8929	1.8737	2.0017	1.9552	1.8804	1.8588	1.8922	1.8631
Na	0.7526	0.6835	0.7452	0.6862	0 6605	0.6777	0.6663	0.6803	0.6668	0.6649
K	0 3823	0.3902	0.3776	0.3900	0.3572	0.3636	0.4160	0.3981	0.4122	0.4086
Cr	0.0012	0.0025	0.0012	0.0025	0.0012	0.0062	0.0025	0.0013	0.0013	0.0013
Total	16.0080	15.9992	16.0075	15.9992	16.0320	16.0180	16.0017	16.0029	16.0076	16.0003
Mg	0.4509	0.1271	0.4421	0.1441	0.4325	0.3123	0.2017	0.1340	0.1870	0.1107

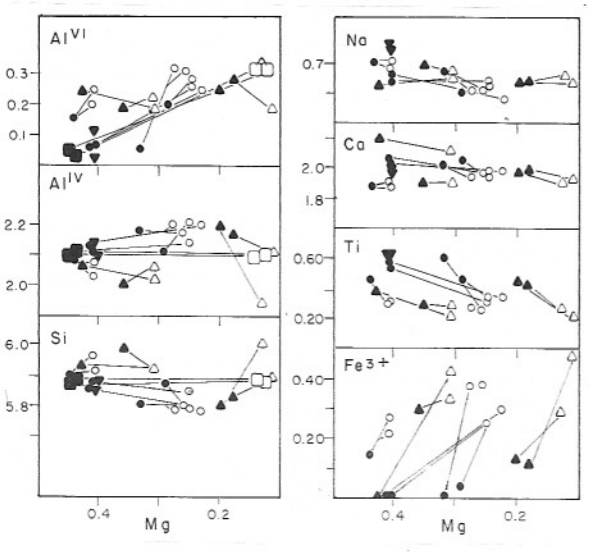

Figure 11 — Elemental correlations of amphiboles with Mg value; symbols as in Fig. 10.

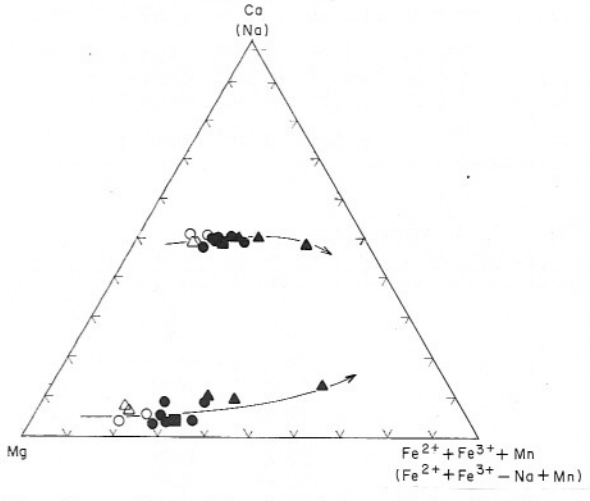

Fig. 12 — Compositional variations of Ca-rich clinopyroxenes; symbols as in Fig. 3.

is a very minor phase in the rocks of Morro Redondo. It mostly occurs as irregular crystals embayed by poikilitic amphiboles.

Compositional variations display a mildly alkaline trend from Ti-salites to Fe-salites (Table 6, Fig. 12) with a concomitant increase in Fe^{2+}, Mn and a decrease in MgO and TiO_2. Na_2O increases towards nepheline syenites (acmite content varies from 5 to 11% in wt) but there is not a strong enrichment as seen in other complexes (Itapirapuã, Gomes *et al.*, 1970; Piratini, Barbieri *et al.*, 1987; see also Gomes *et al.*, 1987). Al^{VI} is low, as expected for low pressure clinopyroxenes. It may be observed that the Mg/Mg + Fe^{2+} of embayed clinopyroxenes is higher than that for coexisting amphiboles suggesting reactions such as: clinopyroxene + evolved Fe- and alkali-rich magma = amphibole, according to petrographic texture. Fe-salite shows a characteristic light green pleochroism in the most evolved rocks.

Biotite

Biotite is present as light yellow to red

Table 6 — Microprobe composition of representative Ca rich pyroxenes from Morro Redondo. FeO* and Fe_2O_3* according to Papike *et al.* (1974). Mg = Mg/Mg + Fe^{3+} + Fe^{2+}. Fe** = Fe^{3+} + Fe^{2+} + Mn. Fe*** = Fe^{3+} + Fe^{2+} + Mn − Na.

	2 Ar	22 Ac	22 Bc	20 Ac	20 Ar	4 A	4 B	3 A	14 A	14 B	11 A	1 A
SiO_2	45.11	49.81	49.89	48.21	48.66	49.23	49.36	48.31	46.59	46.76	49.25	48.46
TiO_2	3.24	1.80	1.47	1.66	0.98	1.48	1.39	1.84	1.60	1.24	1.30	0.71
Al_2O_3	7.93	3.60	3.22	4.39	3.71	3.46	3.31	4.35	5.13	4.90	2.99	3.58
FeO_t	8.20	7.28	7.72	9.59	11.99	9.66	10.79	9.02	11.96	13.68	9.99	17.42
MnO	0.21	0.56	0.54	0.71	1.02	0.77	0.78	0.68	1.04	1.12	0.94	2.73
MgO	11.52	12.99	12.94	10.99	9.44	11.77	10.61	11.68	9.17	8.13	11.38	4.69
CaO	22.20	22.26	22.74	22.54	22.05	22.52	22.65	22.69	21.91	21.72	22.47	20.22
Na_2O	0.74	0.99	0.79	1.06	1.21	0.56	0.62	0.73	1.27	1.26	0.70	1.59
Cr_2O_3	0.01	0.01	0.01	0.01	0.01	0.01	0.01					
Total	99.16	99.30	99.32	99.16	99.07	99.46	99.52	99.30	98.67	98.81	99.02	99.40
Fe_2O_3*	4.37	3.21	3.49	5.02	5.11	2.93	2.27	3.89	6.77	6.52	3.48	3.54
FeO*	4.27	4.40	4.58	5.07	7.39	7.02	8.75	5.52	5.87	7.82	6.86	14.23
Total*	99.60	99.62	99.67	99.66	99.58	99.75	99.75	99.69	99.35	99.46	99.37	99.75
Si	1.6972	1.8604	1.8670	1.8221	1.8591	1.8594	1.8757	1.8221	1.7867	1.8043	1.8713	1.9039
Ti	0.0917	0.0506	0.0414	0.0472	0.0282	0.0420	0.0397	0.0522	0.0461	0.0360	0.0371	0.0210
Al	0.3516	0.1585	0.1420	0.1955	0.1670	0.1540	0.1482	0.1934	0.2319	0.2228	0.1339	0.1658
Fe^{3+}	0.1237	0.0901	0.0984	0.1429	0.1469	0.0833	0.0650	0.1103	0.1952	0.1892	0.0996	0.1047
Fe^{2+}	0.1343	0.1373	0.1432	0.1602	0.2361	0.2218	0.2779	0.1742	0.1883	0.2522	0.2178	0.4676
Mn	0.0067	0.0177	0.0171	0.0227	0.0330	0.0246	0.0251	0.0217	0.0338	0.0366	0.0302	0.0908
Mg	0.6460	0.7231	0.7217	0.6191	0.5376	0.6626	0.6009	0.6566	0.5241	0.4676	0.6445	0.2746
Ca	0.8948	0.8907	0.9117	0.9126	0.9025	0.9112	0.9221	0.9168	0.9002	0.8979	0.9147	0.8510
Na	0.0540	0.0717	0.0573	0.0777	0.0896	0.0410	0.0457	0.0534	0.0944	0.0943	0.0516	0.1211
Cr	0.0003	0.0003	0.0003	0.0003	0.0003	0.0003	0.0003					
Total	4.0003	4.0004	4.0000	4.0002	4.0004	4.0003	4.0007	4.0006	4.0008	4.0008	4.0006	4.0005
Ca	49.5610	47.9153	48.1831	49.1323	48.6239	47.8708	48.7628	48.7774	48.8790	48.7063	47.9691	47.5768
Mg	35.7795	38.9004	38.1446	33.3277	28.9606	34.8076	31.7783	34.9319	28.4607	25.3636	33.7984	15.3526
Fe**	14.6595	13.1843	13.6723	17.5400	22.4155	17.3216	19.4588	16.2907	22.6603	25.9300	18.2326	37.0706
Na	5.9270	7.4039	5.8458	8.2198	9.3983	4.1323	4.7143	5.5441	10.0293	9.9682	5.1973	12.9144
Mg	70.9362	74.6868	73.6142	65.5184	56 3699	66.7718	62.0221	68.1963	55.6732	49.4479	64.9582	29.2859
Fe***	23.1367	17.9093	20.5400	26.2618	34.2318	29.0958	33.2637	26.2596	34.2975	40.5839	29.8445	57.7997
Mg	0.7146	0.7608	0.7492	0.6713	0.5839	0.6847	0.6367	0.6977	0.5774	0.5144	0.6700	0.3243

Table 7 — Microprobe composition of representative biotites from Morro Redondo. Structural formulae calculated on the basis of 22 atoms of O. Mg = Mg/Mg + Fe^{2+}.

	2 A	22 A	22 B	4 A	4 B	4 C
SiO_2	34.54	34.92	34.80	33.66	34.61	33.81
TiO_2	9.38	6.68	6.52	3.96	3.12	3.33
Al_2O_3	15.71	13.88	13.92	14.49	14.48	14.87
FeO_t	10.84	21.52	21.77	27.44	27.28	27.24
MnO	0.09	0.53	0.59	1.36	1.31	1.30
MgO	15.04	9.22	9.17	6.28	7.20	6.38
CaO	0.03					
Na_2O	0.57	0.27	0.21			
K_2O	9.29	9.60	9.65	9.80	9.93	9.84
Total	95.49	96.62	96.63	96.99	97.93	96.77
Si	5.3308	5.6168	5.6073	5.5858	5 6659	5.6115
Ti	1.0886	0.8079	0.7900	0.4941	0.3841	0.4156
Al	2.8574	2 6311	2.6433	2.8338	2.7936	2.9085
Fe^{2+}	1.3990	2.8944	2.9332	3.8077	3.7344	3.7805
Mn	0.0118	0.0722	0.0805	0.1911	0.1816	0 1827
Mg	3.4597	2.2104	2.2022	1.5533	1.7568	1.5782
Ca	0.0050					
Na	0.1706	0 0842	0.0656			
K	1.8289	1.9697	1.9834	2.0745	2.0736	2.0832
Total	16.1516	16.2867	16.3056	16.5404	16.5900	16.5603
Mg	0.7121	0.4330	0.4288	0.2897	0.3199	0.2945

brown pleochroic crystals; it is not an ubiquitous phase, and textural evidence indicates that the biotite crystallised contemporaneously and/or after amphiboles.

Chemically, biotites are better classified as Ti-Fe-biotites, with Ti contents > 0.5 atom per unit formula, and titaniferous Fe-biotites (Ti < 0.5) (Rock, 1982) (Table 7). The Mg value ranges from 43 to 29 and is close to that of the amphiboles. The biotites of sample 2 have Mg values of 71 and higher TiO_2 contents.

Opaque oxides

Magnetite is the only opaque oxide present in the Morro Redondo rocks. It occurs as subhedral to rounded crystals of very early crystallisation, often enclosed by all the other phases.

Ulvospinel contents decrease throughout the sequence (Table 8); abrupt variations from 52% Ulv to nearly zero may be observed in one sample (22). This is probably due to the contemporaneous crystallisation of sphene, that more readily scavenges Ti from the melts. The MnO content is remarkable, as high as 6.75% in some samples, and is not correlated with either Ti or Fe contents.

Table 8 — Microprobe analyses of representative Ti-magnetites from Morro Redondo. FeO* and Fe_2O_3* calculated on ulvospinel basis (Carmichael, 1967).

	2 A	2 B	22 A	22 B	22 C	22 D	20 A	20 B	4 A	4 B	3 A
TiO_2	14.99	14.00	20.87	15.32	12.87	0.07	6.82	2.60	6.00	5.10	10.24
Al_2O_3	4.49	5.19	1.31	4.03	1.14		0.95	0.49	0.76	1.15	1.04
FeO_t	71.74	70.52	72.09	76.41	80.49	92.57	84.62	89.14	86.05	86.16	80.22
MnO	1.21	0.93	1.66	0.01	1.66	0.04	1.94	1.64	1.00	1.68	3.08
MgO	3.56	5.19	0.54		0.21		0.10	0.10	0.18	0.06	0.19
Cr_2O_3	0.05	0.09	0.02	0.03	0.01	0.01		0.02	0.02	0.01	0.01
Total	96.04	95.92	96.49	95.80	96.38	92.69	94.43	93.99	94.01	94.16	94.78
Fe_2O_3*	36.43	38.40	26.87	34.09	43.41	68.52	54.70	63.68	56.34	57.78	47.81
FeO*	38.96	35.96	47.91	45.73	41.43	30.91	35.40	31.84	35.35	34.17	37.20
Total*	99.69	99.77	99.18	99.22	100.73	99.56	99.91	100.37	99.66	99.95	99.57
Ti	3.2623	3.0003	4.7229	3.4474	2.9012	0.0163	1.5619	0.5967	1.3794	1.1686	2.3420
Al	1.5315	1.7432	0.4646	1.4213	0.4028		0.3410	0.1763	0.2738	0.4130	0.3728
Fe^{3+}	7.9327	8.2360	6.0849	7.6768	9.7932	15.9659	12.5355	14.6257	12.9627	13.2477	10.9411
Fe^{2+}	9.4298	8.5709	12.0574	11.4447	10.3847	8.0044	9.0157	8.1269	9.0381	8.7074	9.4621
Mn	0.2966	0.2245	0.4231	0.0025	0.4215	0.0105	0.5004	0.4240	0.2589	0.4336	0.7934
Mg	1.5357	2.2047	0.2422		0.0938		0.0454	0.0455	0.0820	0.0273	0.0861
Cr	0.0114	0.0203	0.0048	0.0071	0.0024	0.0024		0.0048	0.0048	0 0024	0.0024
Total	23.9999	23.9999	23.9999	23.9999	23.9996	23.9995	23.9999	23.9999	23.9999	23.9999	23.9999
Ulv %	42.13	38.93	59.62	44.41	36.57	0.20	19.66	7.49	17.34	14.73	29.50

	3 B	14 A	14 B	11 A	11 B	11 C	1 A	1 B	26 A	26 B
TiO_2	6.12	1.56	0.61	15.35	6.42	1.50	6.16	4.56	7.94	5.74
Al_2O_3	1.40	1.05	0.52	0.53	0.89	1.40	0.99	0.36	0.10	0.22
FeO_t	84.02	89.63	90.73	73.32	84.12	89.73	82.28	84.91	82.94	85.01
MnO	2.32	1.56	1.34	6.75	2.33	0.43	4.42	3.25	3.19	2.88
MgO	0.15	0.10		0.03	0.03	0.05	0.04	0.10		
Cr_2O_3	0.03	0.01			0.01	0.01	0 04		0.03	0.01
Total	94.04	93.91	93.20	95.98	93.80	93.12	93.93	93.18	94.20	93.86
Fe_2O_3*	55.29	65.08	67.14	38.70	55.09	64.14	55.59	59.22	53.21	57.38
FeO*	34.27	31.07	30.31	38.50	34.55	32.02	32.26	31.63	35.06	33.38
Total*	99.58	100.43	99.93	99.86	99.32	99.55	99.50	99.11	99.53	99.61
Ti	1.4029	0.3571	0.1410	3.4959	1.4807	0.3459	1.4173	1.0583	1.8330	1.3262
Al	0.5030	0.3767	0.1884	0.1892	0.3217	0.5060	0.3570	0.1309	0.0362	0.0797
Fe^{3+}	12.6841	14.9070	15.5299	8.8192	12.7147	14.8001	12.7991	13.7527	12.2920	13.2658
Fe^{2+}	8.7354	7.9091	7.7917	9.7507	8.8614	8.2109	8.2533	8.1624	9.0014	8.5764
Mn	0.5990	0.4022	0.3488	1.7314	0.6053	0.1117	1.1454	0.8495	0.8294	0.7494
Mg	0.0682	0.0454		0.0135	0.0137	0.0229	0 0182	0.0460		
Cr	0.0072	0.0024			0.0024	0.0024	0.0097		0.0073	0.0024
Total	23.9999	23.9999	23.9999	23.9999	23.9999	23.9999	23.9999	23.9999	23.9993	23.9999
Ulv %	17.72	4.50	1.77	43.87	18.63	4.37	17.85	13.26	22.93	16.60

DISCUSSION

Systematic variations in both major element chemistry and paragenetic sequences (substitution of clinopyroxene by amphibole and plagioclase by alkali feldspar; plagioclases with calcic cores and alkali feldspars more sodic with evolution; amphibole compositional trends and so on) suggest a genesis by crystal fractionation for the Morro Redondo alkaline complex.

Compositional trends evidenced by variation diagrams and petrography suggest an initial separation of plagioclase + clinopyroxene + amphibole ± biotite ± opaques, sphene and apatite, followed in the final stages of evolution by alkali feldspar fractionation (as also seen by the sharp drop in Sr and Ba abundances), further justifying the transition to the peralkaline field for the most evolved rocks of the complex.

The Morro Redondo samples plot on the potassic side of the feldspar field of the petrogeny's residua system (Fig. 13), and display a trend which is very close to the fractionation curves. It may be noted that the syenitic and alkali syenitic rocks, which are more evolved than microessexite (more Fe-rich clinopyroxenes and amphiboles, less Ca-rich plagioclases and so on), plot very close to the thermal divide, being the most feldspar-rich rocks and confirming their cumulitic nature. Imperfect removal of large alkali feldspar crystals with low density contrast with respect to the host viscous liquid could be the cause for cumulitic textures in the nepheline-bearing syenites.

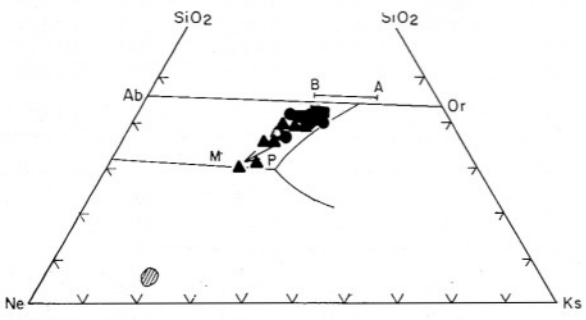

Figure 13 — Phase relations for the petrogeny residua's system (Ne-Ks SiO_2) at 1 kbar of water pressure (after Hamilton & MacKenzie, 1965): normative composition for whole-rocks, nepheline (dashed area) and alkali feldspar compositions (A-B line) are plotted; the arrow denotes the probable liquid line of descent; symbols as in Fig. 3.

The potassic affinity of the rocks also accounts for the compositional trends displayed by the alkali feldspars (tie-lines connecting nephelines with sample 1, lying on the nepheline-feldspar cotectic, intersect the Ab-Or join at a composition very near to Or_{53}), with more potassic cores and more sodic rims. Clear inversion trends for feldspars as envisaged by other authors (Nash *et al.*, 1969; Gittins, 1979) are not evident here.

Mass balance calculations (Stormer & Nicholls, 1978), assuming on petrographic and chemical bases that the most probable liquid line of descent is represented by $22 \rightarrow 14 \rightarrow 1$, indicate that less differentiated nepheline syenites could be produced by 39% fractionation of solid phases consisting of clinopyroxene (5.9%), biotite (12.3%), plagioclase (14.7%), apatite (1.7%), sphene (2.1%) and Ti-magnetite (1.6%), with a res^2 of 0.29. Less satisfactory results ($res^2 = 0.55$) were obtained by utilizing amphibole as a fractionating phase (about 14%). The presence of amphibole considerably reduces plagioclase and biotite fractionation (7.4 and 6.4%, respectively), but gives more consistent results in terms of trace element behaviour, especially for Sr and Ba. In turn, the most evolved nepheline syenites may have been produced by fractionation of 58.6% of solid phases, consisting of alkali feldspar (33.2%), amphibole (8.2%), plagioclase (12.6%), sphene (1.7%), apatite (0.7%) and magnetite (0.5%). This substracted solid shows a chemical composition very close to some nepheline-bearing syenites (e.g. sample 20) affected by feldspar cumulus, confirming that nepheline-bearing syenites and nepheline syenites are cogenetic. This interpretation is also well supported by positive Eu anomalies noticed in the nepheline-bearing syenites.

Table 9 — Calculated and observed trace element abundances for the sequence 22 through 1 (k_d from Cullers & Medaris, 1977; Kyle, 1981; Irving & Price, 1981; Aurisicchio *et al.*, 1983; Worner *et al.*, 1983; Irving & Frey, 1984).

	obs	calc		obs	calc
Ba	72	82	Nd	35	35
Rb	155	155	Sm	4.6	4.7
Sr	372	397	Eu	1.2	1 4
Zr	525	494	Gd	2.6	3.8
La	110	102	Yb	2.9	1.8

The correspondence between observed and calculated values for trace elements, using Rayleigh model, percentages of fractionating phases and liquid fraction values obtained from major element mass balances, is generally good (Table 9).

SUMMARY AND CONCLUSIONS

The alkaline intrusive complex of Morro Redondo is substantially composed of syenites and nepheline syenites, probably emplaced 73 Ma ago into the Precambrian basement.

Mineralogic, geochemical and petrographic data strongly support a cogenetic affinity for the intrusive rocks, due to "in situ" differentiation by crystal fractionation and/or accumulation in a shallow chamber with increasing water pressures, as hypothesized by Valença *et al.* (1983).

The Morro Redondo rocks show a noteworthy potassic affinity that, on the basis of petrographic and petrochemical characteristics

Table 10 — Rb, Sr and Sr isotopic ratio (measured and initial) for some samples of the Morro Redondo intrusive complex. Sr separation was achieved by ion-exchange standard chromatographic methods and isotopic analyses were carried out by a VG 354 thermal ionization double-collector mass spectrometer (University of Naples); precision is espressed as two-sigma; accuracy was checked by repeated analyses of NBS 987 standard (0.71026 ± 1) during the analytical work.

Sample	Rb (ppm)	Sr (ppm)	$(^{87}Sr/^{86}Sr)_m$	2 δ	$(^{87}Sr/^{86}Sr)_o$	$^{87}Rb/^{86}Sr$
20	115	3817	0.70558	1	0.70549	0.09
15	158	1964	0.70551	1	0.70527	0.23
4	116	3141	0.70567	1	0.70556	0.10
2	125	1784	0.70510	1	0.70491	0.20
12	115	1078	0.70573	1	0.70542	0.30
11	129	2214	0.70566	1	0.70549	0.16
8	127	287	0.70603	1	0.70550	0.51
1	131	372	0.70651	1	0.70548	0.99
26	160	445	0.70630	1	0.70525	1.01

obtained up-to-now, is tentatively linked to other alkaline complexes cropping out in the Rio de Janeiro State (Itatiaia, Itaúna, Morro de São João, Passa Quatro, Rio Bonito, Soarinho, Tanguá) and also in the littoral of São Paulo (Ilha de Vitória). Another group of intrusions is typically sodic in character and clusters around Jacupiranga (Banhadão, Itapirapuã, Juquiá, Tunas and so on), but also includes complexes far from this area such as Anitápolis, Lages and Piratini. Most of them have carbonatites as main rock type.

Initial Sr isotopic ratios range from 0.70491 to 0.70556 (Table 10). They suggest a subcrustal origin for the parental magmas from which the "syenitic" rocks of the complex were differentiated and, probably, different parental magmas for the dykes, considering the relatively low $^{87}Sr/^{86}Sr$, the petrographic and geochemical characteristics of sample 2. Extrapolating the liquid line of descent back towards more femic magmas, these may have been of basanitic affinity. No substantial contribution by radiogenic crustal Sr was observed, taking into account the very high Sr content of the rocks.

ACKNOWLEDGEMENTS

Thanks are due to the Brazilian (FINEP — Proc. 43.88.0690.00 and FAPESP — Procs. 88/1214-0 and 88/0049-6, grants to C.B. Gomes) and Italian (MPI, grant 1987 to L. Morbidelli) agencies for financial support. The authors are also indebted to Dr. T.R. Fairchild for reviewing the manuscript. L. Melluso greatly acknowledges Dr. L. Civetta for the facilities in the use of the isotope geochemistry laboratory of the University of Naples.

REFERENCES

AURISICCHIO, C.; BROTZU, P.; MORBIDELLI, L.; PICCIRILLO, E.M.; TRAVERSA, G. (1984) Basanite to peralkaline phonolite suite: quantitative crystal fractionation model (Nyambeni range, East Kenya Plateau). N. Jb. Mineral, Abh., **148**:113-140.

BARBIERI, M.; BECCALUVA, L.; BROTZU, P.; CONTE, A.; GARBARINO, C.; GOMES, C.B.; LOSS, E.L.; MACCIOTTA, G.; MORBIDELLI, L.; SCHEIBE, L.F.; TAMURA, R.M.; TRAVERSA, G. (1987) Petrological and geochemical studies of alkaline rocks from continental Brazil. 1. The phonolite suite from Piratini, RS. Geochim. Brasil., **1**:109-138.

BARTH, T.F. (1963) The composition of nepheline. Schweiz. Mineral. Petr. Mitt., **43**:153-164.

BEDARD, J.H. (1988) Comparative amphibole chemistry of the Monteregian and White Moutain alkaline suites, and the origin of amphibole megacrysts in alkalic basalts and lamprophyres. Mineral. Mag., **52**:91-103.

BOYNTON, W.V. (1984) Cosmochemistry of the rare earth elements: meteorite studies. In: P. Henderson (ed.) Rare earth element gheochemistry. Elsevier, p. 63-114.

BROTZU, P.; BECCALUVA, L.; CONTE, A.; FONSECA, M.; GARBARINO, C.; GOMES, C.B.; MACCIOTTA, G.; MANSUR, R.L.; MELLUSO, L.; MORBIDELLI, L.; RUBERTI, E.; SIGOLO, J.B.; TRAVERSA, G.; VALENÇA, J.B. (1988) Petrological and geochemical studies of alkaline rocks from continental Brazil. 5. The Morro Redondo alkaline complex, State of Rio de Janeiro. Int. Conf. "Geochemical evolution of the continental crust", Poços de Caldas, Brazil, p. 97-103.

CARMICHAEL, I.S.E. (1967) The iron-titanium oxide minerals of salic volcanic rocks and their associated ferro-magnesian silicates. Contrib. Mineral. Petrol., **14**:36-54.

CULLERS, L. & MEDARIS, G. (1977) Rare earth elements in carbonatite and cogenetic alkalic rocks: examples from Seabrook Lake and Callander Bay, Ontario. Contrib. Mineral. Petrol., **65**:143-153.

DE LA ROCHE, H.; LETERRIER, P.; GRANDCLAUDE, P.; MARCHAL, E. (1980) A classification of volcanic and plutonic rocks using R1-R2 diagram and major element analyses. Its relationships with current nomenclature. Chem. Geol., **29**:183-210.

DOLLASE, W.A. & THOMAS, W.M. (1978) The crystal chemistry of silica-rich, alkali-deficient nepheline. Contrib. Mineral. Petrol., **66**:311-318.

GHIORSO, M.S. (1984) Activity-composition relations in the ternary feldspars. Contrib. Mineral. Petrol., **87**:282-296.

GITTINS, J. (1979) The feldspathoidal alkaline rocks. In: H.S. Yoder Jr. (ed.) The evolution of igneous rocks. Princeton Univ. Press, p. 351-390.

GOMES, C.B.; MORO, S.L.; DUTRA, C.V. (1970) Pyroxenes from the alkaline rocks of Itapirapuã, São Paulo, Brazil. Amer. Mineral., **55**:224-230.

GOMES, C.B.; BARBIERI, M.; BECCALUVA, L.;

BROTZU, P.; CONTE, A.; GARBARINO, C.; MACCIOTTA, G.; MELLUSO, L.; MORBIDELLI, L.; SCHEIBE, L.F.; TAMURA, R.M.; TRAVERSA, G. (1988) Petrological and geochemical studies of alkaline rocks from continental Brazil. 2. The Tunas massif, state of Paraná. Geochim. Brasil., **1**:201-234.

HAMILTON, D.L. (1961) Nephelines as crystallization temperature indicators. J. Geol., **69**:321-329.

HAMILTON, D.L. & MacKENZIE, W.S. (1965) Phase equilibrium studies in the system $NaAlSiO_4$(nepheline)-$KAlSiO_4$(kalsilite)-SiO_2-H_2O. Mineral. Mag., **34**:214-231.

HENDERSON, C.M.B. & GIBB, F.G.F. (1983) Felsic mineral crystallization trends in differentiating alkaline basic magmas. Contrib. Mineral. Petrol., **84**: 355-364.

IRVING, A.J. & FREY, F.A. (1984) Trace element abundances in megacrysts and their host basalts: constraints on partition coefficients and megacrysts genesis. Geochim. Cosmochim. Acta, **48**:1201-1221.

IRVING, A.J. & PRICE, R.C. (1981) Geochemistry and evolution of lherzolite-bearing phonolitic rocks from Nigeria, Australia, East-Germany and New Zealand. Geochim. Cosmochim. Acta, **45**:1305-1320.

KUDO, A.M. & WEILL, D.F. (1970) An igneous plagioclase geothermometer. Contrib. Mineral. Petrol., **25**:52-65.

KYLE, P.R. (1981) Mineralogy and geochemistry of a basanite to phonolite sequence at Hut Point Peninsula, Antarctica, based on core from Dry Valley Drilling Project, Drill-holes 1, 2 and 3. J. Petrol., **22**-451-500.

LAMEGO, A.R. (1936) O maciço de Itatiaia e regiões circundantes. Depto. Nac. Prod. Min., S.G.M., **88**, 93p.

LE BAS, M.J.; LE MAITRE, R.W.; STRECKEISEN, A.; ZANETTIN, B. (1986) A chemical classification volcanic rocks based on the Total Alkali-Silica diagram. J. Petrol., **27**:745-750.

LEAKE, B.E. (1978) Nomenclature of amphiboles. Mineral. Mag., **42**:533-563.

MATHEZ, E.A. (1973) Refinement of the Kudo-Weill plagioclase thermometer and its application to basaltic rocks. Contrib. Mineral. Petrol., **41**:61-72.

NASH, W.P.; CARMICHAEL, I.S.E.; JOHNSON, R.W. (1969) The mineralogy and petrology of Mt. Suswa, Kenya. J. Petrol., **10**:409-439.

PAPIKE, J.J.; CAMERON, K.L.; BALDWIN, K. (1974) Amphiboles and pyroxenes: characterization of other than quadrilateral components and estimates of ferric iron from microprobe data. Geol. Soc. Am. Abstracts with Programs, **6**:1053-1054.

RIBEIRO FILHO, E. & CORDANI, U.G. (1966) Contemporaneidade das intrusões de rochas sieníticas do Itatiaia, Passa Quatro e Morro Redondo. XX Congr. Bras. Geol., Resumos, **1**:62-63.

ROCK, N.M.S. (1982) Chemical mineralogy of the Monchique alkaline complex, Southern Portugal. Contrib. Mineral. Petrol., **81**:64-78.

SAGGERSON, E.P. & WILLIAMS, L.A.S (1964) Ngurumanite from Southern Kenya and its bearing on the origin of rocks in the Northern Tanganyika alkaline district. J. Petrol., **5**:40-81.

STEIGER, R.H. & JAEGER, E. (1977) Subcommission on geochronology: conventions on the use of decay constants in geochronology and cosmochronology. Contributions to the geologic time scale. A.A.P.G. Studies in geology, **6**:67-71.

STORMER Jr., J.C. (1975) A practical two-feldspar geothermometer. Amer. Mineral., **60**:667-674.

STORMER Jr., J.C. & NICHOLLS, J. (1978) XL Frac: a program for the interactive testing of magmatic differentiation models. Comput. Geosci., **4**:143-159.

STRECKEISEN, A. (1976) To each plutonic rock its proper name. Earth Sci. Rev., **12**:1-32.

VALENÇA, J.G. (1980) Geology, petrography and petrogenesis of some alkaline igneous complexes of Rio de Janeiro State, Brazil. PhD Thesis, University of Western Ontario, 248p. [unpuplished].

VALENÇA, J.G.; REIS, A.P.; CARVALHO FILHO, C. A.; SOARES FILHO, J.R.S.; BRAUN, P.V.C.B. (1983) Geologia do complexo ígneo alcalino do Morro Redondo (Município de Resende, Estado do Rio de Janeiro). An. Acad. brasil. Ci., **55**:135-136.

WORNER, G.; BEUSEN, M.; DUCHATEAU, H.; GIJBELS, R.; SCHMINCKE, H.U. (1983) Trace element abundances and mineral-melt distribution coefficients in phonolites from the Laacher See Volcano (Germany). Contrib. Mineral. Petrol., **84**:152-173.